Downregulation of IQGAP2 Correlates with Prostate Cancer Recurrence and Metastasis[1]

Yanyun Xie, Linfeng Zheng and Lijian Tao

Division of Nephrology, Xiangya Hospital, Central South University, Hunan, Changsha, China

Abstract

IQGAP2 was recently reported as a tumor suppressor of prostate cancer (PC). Nonetheless, its clinical implications remain unknown. To address this issue, we extracted data related to IQGAP2 mRNA expression and genomic alterations from multiple large datasets within the Oncomine and cBioPortal databases and performed *in silico* analyses to determine a potential association of IQGAP2 mRNA expression and its genomic alterations with PC progression. In 4 cohorts consisting of 118 normal prostate tissues and 277 PCs, IQGAP2 mRNA expression was significantly elevated particularly in low-grade (primary Gleason score ≤3) PCs; these changes separate PC from normal tissues with area under curve values of 0.7-0.8. Significant reductions in IQGAP2 mRNA levels and gene copy number occurred in more than 70 metastases compared to at least 230 local PCs. This duo-alteration in IQGAP2 expression supports IQGAP2 elevation suppressing and its downregulation facilitating PC progression. Deletion and missense mutations were detected in 23 of 492 primary PCs; these alterations significantly associate with PC recurrence (HR=2.71; 95% CI: 1.35-5.44; P=.005) after adjusting for known risk factors and correlate with reductions in disease-free survival (DFS, P=.002). *IQGAP2* (5q13.3) genomic alterations were observed in SPOP-marked PCs and co-occurred with deletion in the *RN7SK* (16p12.2), *SNORA50A* (16q21), and *SNORA50C* (17q23.3) genes; the co-occurrence associated with reductions in DFS (P=4.14e-4). In two independent PC populations, MSKCC (n=130) and TCGA provisional (n=490), reductions in IQGAP2 mRNA expression were significantly associated with DFS. Collectively, this investigation reveals an association of IQGAP2 with PC progression.

Translational Oncology (2019) 12, 236–244

Introduction

Prostate cancer (PC) is the most frequently diagnosed male malignancy and the second leading cause of cancer-related deaths for men living in the developed countries [1]. The disease progresses from high-grade prostatic intraepithelial neoplasia to invasive carcinoma and then to metastatic tumors with bone being the primary site [2]. Local tumors are effectively managed through watchful waiting, surgery, and radiation. Approximately one-third of patients will experience biochemical recurrence (BCR) [3], a condition with increasing risk of developing castration-resistant prostate cancer (CRPC) and metastasis [4]. Metastatic PCs remain incurable. Improving our understanding of the mechanisms responsible for PC progression is of critical importance in management of prostate cancer.

The IQ motif GTPase-activating proteins (IQGAPs) consist of IQGAP1, IQGAP2, and IQGAP3. These proteins share the identical structural features including a CHD (calponin homology domain), WW, IQ, GRD (RasGAP-related domain), RGCT (RasGAP_C terminus), and aPI (atypical phosphatidylinositol (3,4,5) binding) domain. Except

the WW motif, these domains are highly conserved among IQGAPs with homology ranging from 60% to 93% [5–8]. While individual IQGAP proteins contribute to diverse physiological processes involving the kidney, brain, heart, pancreas, and lung [9], they all bind Cdc42 and Rac1 GTPase [6,10,11], supporting the existence of highly homologous domains in IQGAPs. However, IQGAP1 and IQGAP3 (particularly IQGAP1) activate the Ras-MAP kinase pathways, receptor tyrosine kinases, Wnt, and other signaling pathways [6,11–13]. Likewise,

Address all correspondence to: Yanyun Xie, 87 Xiangya Road, Changsa, Hunan 410008, China. E-mail: xieyanyun999@hotmail.com

accumulative evidence reveals an oncogenic role of IQGAP1 in multiple tumorigenic processes [9,12].

Despite being 62% identical and having an even higher level of homology to the respective IQGAP1 motifs (except the WW domain) [8,11], IQGAP2 suppresses the tumorigenesis of hepatocellular carcinoma (HCC) [14–16] and gastric cancer [8,17]. Loss of IQGAP2 in the mouse liver resulted in activation of the Wnt/β-catanin pathway [15]. Of note, IQGAP2 enhanced E-cadherin expression and repressed Akt activation in PC cells and displayed tumor suppression activity toward PC [8,18]. However, the contributions of IQGAP2 to suppression of PC tumorigenesis need to be further studied.

To further investigate IQGAP2-medaited suppression of PC tumorigenesis, we took advantage of the rapid development in profiling of gene expression and study of cancer genomic alterations which result in deposition of a large amount of raw data into well-organized databases Oncomine (Compendia Bioscience, Ann Arbor, MI) and cBioPortal [19,20] (http://www.cbioportal.org/index.do) by extraction and analysis of data relevant to IQGAP2 mRNA expression and genomic alterations. We report here alterations in IQGAP2 correlating with PC tumorigenesis, recurrence, and metastatic.

Materials and Methods

Oncomine

The Oncomine (Compendia Bioscience, Ann Arbor, MI; www.onocomine.org) database contains publicly available microarray data on multiple tumor types. We have extracted IQGAP2 mRNA expression data from four datasets: the Taylor, Grasso, Lapointe, and Tomlins datasets [21–24]; data related to IQGAP2 gene copy number (GCN) variations were obtained from the Taylor and Grasso datasets [21,22]. The mRNA data were reported as Log2 Median-Centered ratio, and DNA copy number data were expressed as Log2 copy number units in the Oncomine database.

cBioPortal

The database consists of 146 sets of cancer genomic data. A variety of tools are also provided to analyze genomic alterations with respect to enrichment and association with disease-free survival (DFS) and overall survival (OS). Comprehensive clinical information is available. cBioPortal [19,20] contains 11 PC genomic datasets covering primary PC, CRPC, and metastasis (http://www.cbioportal.org/index.do). We have analyzed all PC datasets with focus on the largest one (TCGA provisional) containing 492 primary PCs with sequencing and gene copy number variation (CNV) determined. Clinical information for all 492 patients was downloaded for Cox regression analyses.

Cutoff Point Determination

Cutoff point of IQGAP2 mRNA expression in separation of recurrent PC was performed with Maximally Selected Rank Statistics (the *Maxstat* package) in R.

Statistical Analysis

Statistical analyses for data extracted from Oncomine were performed using GraphPad Prism 5 software. A *P* value <.05 was
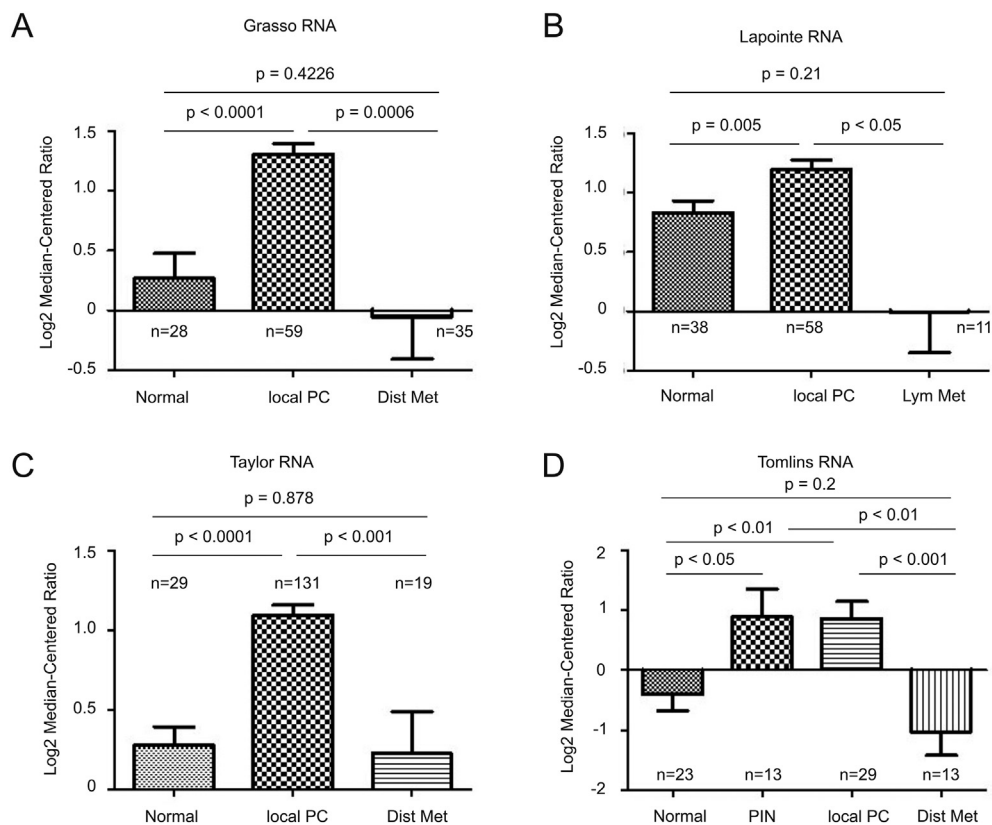

Figure 1. Changes in IQGAP2 mRNA expression during prostate cancer tumorigenesis and metastasis. IQGAP mRNA expression data were extracted from the Grasso (A), Lapointe (B), Taylor (C), and Tomlins (D) datasets within the Oncomine (Compendia Bioscience, Ann Arbor, MI) database and analyzed. Means±SD are graphed. Statistical analyses were performed using a two-tailed Student's *t* test. Dist Met: distant metastasis; lym met: lymph metastasis

considered statistically significant. Kaplan-Meier surviving curves and log-rank test were used to analyze DFS and OS (cBioPortal) for data related to genomic changes. Kaplan-Meier surviving curves and log-rank test were also performed using the R survival package. Univariate and multivariate Cox proportional-hazards regression analysis was performed using SPSS Statistics 23.

Results

A Two-Phase Alteration in IQGAP2 mRNA Expression Following PC Tumorigenesis and Metastasis

IQGAP2 was recently suggested to possess a tumor surveillance activity towards PC tumorigenesis without detailed knowledge on IQGAP2 alterations in primary PCs [18]. To examine these changes, we took advantage of the available resource of large sets of PC gene expression raw data deposited in Oncomine, and extracted the data related to IQGAP2 mRNA expression from the Grasso, Lapointe, Taylor, and Tomlins datasets [21–24] within the database. In these four independent patient cohorts that consist of 188 normal prostate tissues and 277 local PCs, significant increases in IQGAP2 mRNA expression were commonly detected (Figure 1, A-D). An elevation of IQGAP2 mRNA level in prostatic intraepithelial neoplasia (PIN), precancerous lesions, over normal prostate tissues was also detected (Figure 1D). We have subsequently separated PCs into low-grade tumors with primary Gleason score (GS) ≤3 and high-grade carcinomas with primary GS 4-5. A trend reduction in IQGAP2 mRNA expression was observed in high-grade PCs compared to low-grade PCs in three independent patient cohorts (Supplementary Figure 1). These observations are in accordance with the reported changes in IQGAP2 protein expression in PINs and low- and high-grade PCs, a study involving a limited number of patients (16 normal prostate tissues, 12 PINs, 21 low-grade and 26 high-grade tumors) [18]. Considering IQGAP2-associated tumor suppression activity towards PC tumorigenesis, an elevation of IQGAP2 expression in PINs and low-grade PCs is likely for repression of tumorigenesis [18], and its downregulation may ensure PC progression. This possibility is further supported by a dramatic reduction of IQGAP2 mRNA in lymph node (Figure 1B) and distant metastases (Figure 1, A, C, and D) from local PCs. The levels of IQGAP2 mRNA in metastases are no longer higher or likely lower than in normal prostate tissues (Figure 1, A-D).

The reduction of IQGAP2 mRNA expression in metastasis is in part attributable to decreases in IQGAP2 GCN. In two independent patient cohorts (Grasso and Taylor), significant decreases in IQGAP2 GCN were detected in 72 metastases compared to 238 local PCs (Figure 2, A and B).

An association of the early phase of IQGAP2 elevation with PC tumorigenesis

Since the early-phase increases in IQGAP2 are likely to counter PC progression, we reasoned that the elevation may have some clinical applications. In line with this possibility, increases in IQGAP2 mRNA expression separate prostate carcinomas from normal prostate tissues with accuracy ranging from 0.7 to 0.8 as measured by area under the curve (AUC) of receiver operating characteristics (ROC) curves; similar results were obtained from four independent patient cohorts: the Grasso, Lapointe, Taylor, and Tomlins (Figure 3, A-D).

Genomic Alterations in the IQGAP2 Gene as an Independent Risk Factor for PC Recurrence

The observed reductions in IQGAP2 GCN (Figure 2) reveal genomic alterations in the IQGAP2 gene. To further examine IQGAP2-associated genomic alterations, we extracted data related to IQGAP2 genomic changes from all datasets within the cBioPortal database (http://www.cbioportal.org/index.do). Deep deletion or homodeletion was observed in 6.7% (4/59) of metastatic adenocarcinomas (MICH cohort) [22], 4.3% (21/492) of primary PCs (TCGA), and 1.8% (1/56) of 56 primary PCs (Broad/Cornell cohort, 2013) [25]. Mutations in the IQGAP2 gene were observed in 0.4% (2/492) of primary PCs (TCGA), 1.3% (2/150) of PC metastases (SU2C) [26], and 0.9% (1/109) of PCs (Broad/Cornell cohort, 2012) [27] (Supplementary Table 1).

The TCGA (provisional) cohort is the most comprehensive one with 492 primary PCs that have been sequenced and gene CNV determined; the cohort also has the most number of cases with IQGAP2 genomic alterations: 23 tumors with either IQGAP2 homodeletion (21 cases) or mutation (2 cases) (Figure 4A, Supplementary Table 1). We thus focused our analyses on this cohort. Among 23 tumors with the IQGAP2 genomic alterations (Figure 4A), 22 have follow-up data and are enriched with PC recurrence (10/22=45.5%) in comparison to the tumor population without the alterations (79/463=17.1%) (Figure 4B); importantly, the alterations significantly correlated with a reduction in DFS (Figure 4B). Furthermore, two patients with metastatic and IQGAP2 deleted PC died in 33 and 70 months, respectively, while the time reaching 50% of deaths in 47 patients with metastatic PCs without IQGAP2 deletion was 97 months (P=.0747, Supplementary Figure 2).

Our previously reported reductions of the IQGAP2 protein [18] and the currently observed decreases in IQGAP2 mRNA in high-grade PCs
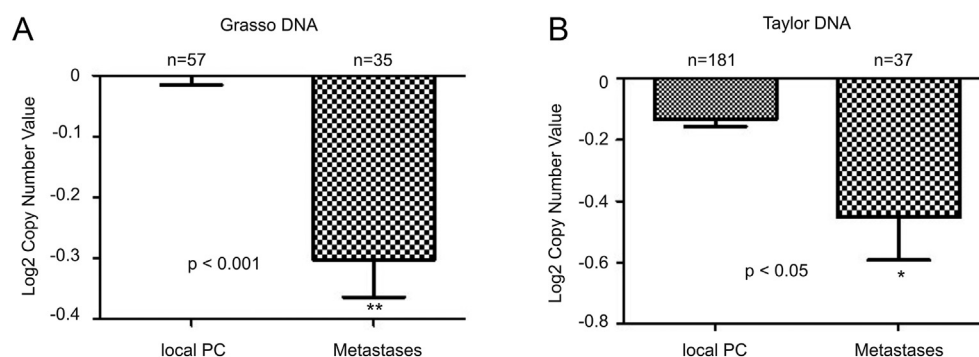
Figure 2. Reductions in *IQGAP2* GCN in PC metastases. *IQGAP2* gene copy variation data were extracted from the Grasso (A) and Tayor (B) datasets within the Oncomine database. Means±SD are graphed. Statistical analysis was performed using two-tailed Student *t*-test.
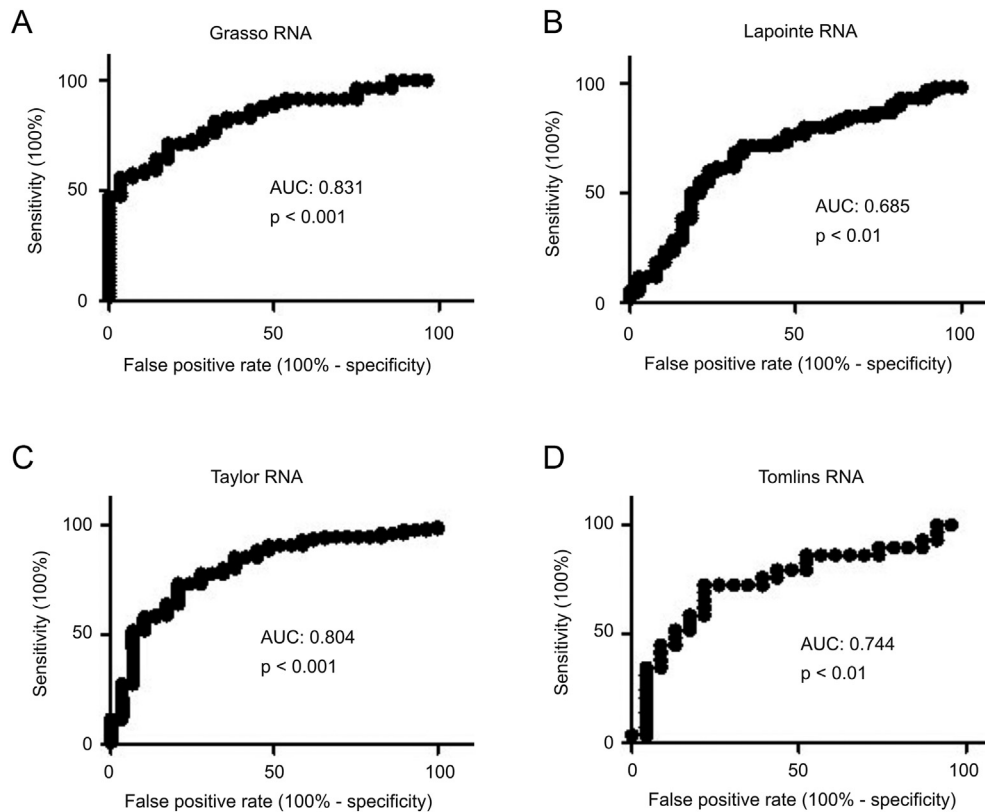
Figure 3. Elevations in IQGAP2 mRNA level in primary PC separate prostate carcinomas from normal prostate tissues. IQGAP mRNA expression data were extracted from the Grasso (A), Lapointe (B), Taylor (C), and Tomlins (D) datasets within Oncomine (Compendia Bioscience, Ann Arbor, MI). The respective ROC curves of primary PC versus normal prostate tissues were calculated.

(Supplementary Figure 1) indicate that *IQGAP2* genomic alterations should occur in high-grade PCs. The TCGA cohort consists of 196 PCs with primary GS ≤3 and 289 PCs with primary GS 4-5 (Supplementary Table 2); 19 of 22 tumors with the aforementioned *IQGAP2* genomic alterations are in high-grade tumors (P=.0128; Supplementary Table 2). These observations further support the correlation of *IQGAP2* genomic changes with reduction in DFS (Figure 4B).

PCs with *IQGAP2* gene homodeletion and mutation are associated with PC recurrence with a hazard ratio (HR) value of 2.68 (95% CI: 1.389-5.186, P=.003) (Table 1). After adjusting for known risk factors (TNM stage, extraprostatic extension, age at diagnosis, primary GS, and surgical margin), the genomic changes remain a risk factor for PC recurrence (HR=2.71, 95% CI: 1.347-5.435, P=.005) (Table 1). While the PSA levels at diagnosis are not available, the TCGA cohort includes the most recent PSA for 428 patients. In this patient group, univariate Cox regression analysis revealed the associated risk for PC recurrence for IQGAP2 genomic alterations being HR=2.74 (95% CI: 1.414-5.309, P=.003) and for the most recent PSA being HR=1.049 (95% CI: 1.018-1.081, P=.002); after adjusting for the PSA levels, IQGAP2 genomic alterations correlate with PC recurrence with an HR value of 2.502 (95% CI: 1.265-4.947, P=.008); after adjusting for the above risk factors together with the PSA levels, the risk of developing PC recurrence in patients with IQGAP2 genomic alterations is HR=2.80 (95% CI: 1.384-5.672, P=.004) (data not shown). Collectively, homodeletion and mutations in the *IQGAP2* gene are an independent risk factor for PC recurrence.

IQGAP2-Associated Co-Occurrence in Gene CNVs and Their Correlation with PC Recurrence

Human IQGAP2 resides at 5q13.3. We have thus examined the top genes that are located in other chromosomes and with concurrent gene CNV alongside the *IQGAP2* genomic alterations. We notice three noncoding small RNA genes in this regard (Table 2, Figure 5A). SNORA50A and SNORA50C are small nucleolar RNA, H/ACA Box 50A and C with function unknown (PubMed). RN7SK is a small nuclear RNA; it downregulates transcription via inhibiting Cdk9/cyclin T-mediated phosphorylation of the RNA polymerase II C-terminal domain [28,29]. RN7SK will thus likely inhibit cell proliferation.

While the functionality of the co-alterations remains to be elucidated, the co-occurrence of genes residing in different chromosomes (Table 2, Figure 5A) suggests its clinical significance. Indeed, changes in this group of genes (Figure 5A) robustly correlate with reductions in DFS (Figure 5B); the changes are a risk factor for PC recurrence (HR: 2.67, 95% CI: 1.507-4.726, P=.001) and an independent factor after adjusting for TNM stage, extraprostatic extension, age at diagnosis, primary GS, and surgical margin with an HR of 2.414 (95% CI: 1.317-4.425, P=.004).

Clustering of IQGAP2 mutations at its C-terminus

There are four missence and one missense+frame shift (fs) mutations detected in three PC datasets within cBioPortal: A1329V and V1557L in primary PC (TCGA), K1177Nfs*25 and L1236F in metastases (SU2C), and K1532Q in primary PC (Broad/Cornell, 2012) (Supplementary Table 1, Figure 6A). Both K1177Nfs*25 and
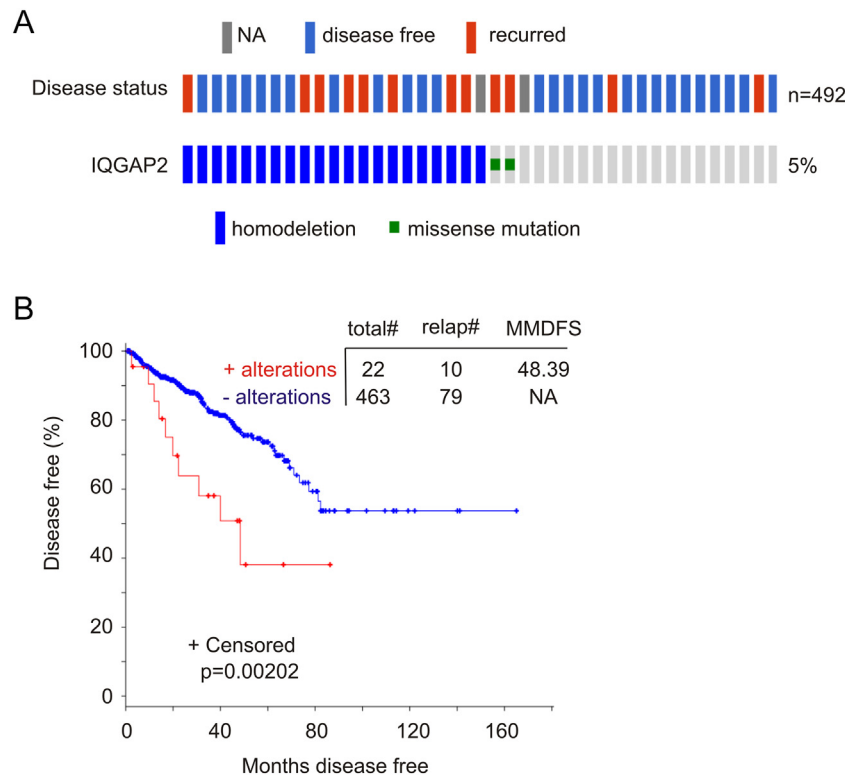
Figure 4. Genomic alterations in the *IQGAP2* gene associate with a reduction in DFS. Data were extracted from the TCGA dataset within the cBioPortal database [19,20]. (A) Deep deletion (homodeletion) and missense mutations in the *IQGAP2* gene are indicated. Disease status is also included. Each individual bar represents a single patient. The cohort contains 492 tumors with genomic sequence and gene CNVs determined. Only those patients with IQGAP2 genomic alterations and a limited number of patients without the alterations are shown. (B) DFS in patients with and without *IQGAP2* genomic alterations in their tumors was analyzed using Kaplan-Meier survival curve. Statistical analysis was performed using log-rank test. Total#: total number of cases; relap#: number of relapsed cases; MMDFS: median months of disease-free survival; NA: not available. Censored individuals are indicated; the number of censored individuals is the total individuals minus relapsed patients.

L1236F occur in the GRD domain of (Figure 6A), and L1236F is detected in the newly identified Ex domain (residues 1204-1246) of IQGAP2 (Figure 6A) that provides an additional binding site for Cdc42 [30]. While A1329V is in an N-terminal region adjacent to

Table 1. Univariate and Multivariate Cox Regression Analysis for the DFS in PC Patients

Clinical Variables	n^*	Univariate			Multivariate		
		HR	CI (95%)	*P* Value	HR	CI (95%)	*P* Value[#]
IQGAP2 Alt[†]							
0	462						
1	23	2.684	1.389-5.186	0.003	2.706	1.347-5.435	0.005
TNM stage[‡]							
I or II	189						
III or IV	296	3.398	1.945-5.934	<0.0001	2.218	1.197-4.110	0.011
Extra Pro Ext[§]							
0	183						
1	13	1.58	0.49-5.089	0.444	0.935	0.599-1.461	0.769
Age at diagnosis	473	1.025	0.993-1.508	0.135	0.996	0.963-1.030	0.802
Primary GS	473	2.424	1.747-3.361	<0.0001	1.841	1.264-2.683	0.001
Margin status[¶]							
0	310						
1	146	1.337	0.324-5.519	0.688	1.997	0.480-8.315	0.342

* Number of indicated cases.
† Genomic alterations (homodeletion and mutation) in the IQGAP2 gene.
‡ Six cases with stage not available have been grouped in the I or II category.
§ Extraprostatic extension; there were 289 cases with the extension status not available (NA).
¶ Surgical margin status; 2 cases marked unknown (N), 10 cases with the status NA, and 16 cases were Rx.
# *P* values were derived from multivariate Cox regression with other factors adjusted.

the RGCT domain (Figure 6A), both K1532Q and V1557L are in the aPI domain (Figure 6A), a motif required for the associaiton of IQGAP2 with cell membrane [7]. Except for K1177 that is conserved among IQGA1-3, other four residues, L1236, A1329, K1532, and V1557, are unique to IQGAP2 (Figure 6B). Among these mutants, A1329V and V1557L were detected in recurred PCs (Figure 6A), while K1177Nfs*25 and L1236F occurred in bone metastases (Supplementary Table 1, footnote 7). Collectively, evidence suggests that the clustering of these mutations in the C-terminal region (Figure 6A) impairs IQGAP2 function.

Inclusion of prostate carcinomas with the IQGAP2 genomic alterations within the SPOP subtype

Genomic alterations generally group PCs into the ETS gene fusion, in which the TMPRSS3-ERG fusion is the prodominant subtype, and the *SPOP*, *FOXA1*, or *IDH1* mutation family [31]. The SPOP mutations and ERG rearrangement occur in a mutually exclusive manner [27,32]. Importantly, SPOP functions in the homologous recombination-based repair of double-strand DNA breaks [33]; its mutations will resuslt in genome instability. With this knowledge, we found a robust enrichment between *IQGAP2* genomic changes and *SPOP* mutations (Table 2, Figure 7). SPOP mutations commonly co-occur with a loss of the *MAP3K7* and *CHD1* genes [27,32]. In this regard, alterations in the *IQGAP2* gene occur alongside homodeletions and mutations in both *MAP3K7* and *CHD1* genes

Table 2. The Co-Occurrence of Copy Number Alteration with IQGAP2 Genomic Alterations[*]

Gene	Locus	Altered Group	Unchanged Group	Log $R^†$	P Value	q Value
SNORA50C	17q23.3	20 (86.96%)[‡]	6 (1.28%)[§]	6.09	2.05e-27	6.08e-25
SNORA50A	16q21	20 (86.96%)	9 (1.92%)	5.5	8.74e-26	1.7e-23
RN7SK	6p12.2	20 (86.96%)	10 (2.13%)	5.35	2.61e-25	4.82e-23
SPOP	17q21.33	16 (69.57%)	39 (8.32%)	3.06	9.42e-12	1.05e-7

P values were determined by Fisher exact test (cBioPortal).
q values were derived from Benjamini-Hochberg procedure (cBioPortal).
[*] IQGAP2 genomic alterations include homodeletion and missense mutations.
[†] Log2-based ratio of percentage in altered group/percentage in unchanged group.
[‡] Number of cases with CNV/number of cases with IQGAP2 genomic alterations (23) × 100; for example, the % for SNORA50C is 20/23 × 100 = 86.96%.
[§] Number of cases with CNV/case numbers without IQGAP2 genomic alterations (492 − 23=469); for example, the % for SNORA50C is 6/469 × 100 = 1.28%.

($P<.001$; log odds ratio >3) (Figure 7). Furthermore, *IQGAP2* genomic changes do not display co-occurance with either FOXA1 ($P=.136$) or IDH1 ($P=.062$) genomic alterations (amplification, deletion, and mutation).

Correlation of Reductions in IQGAP2 mRNA Expression with PC Recurrence

IQGAP2 possesses tumor suppression activity towards PC [8,18], indicative of an association of IQGAP2 downregulation with poor prognosis of patients with PC. To test this possibility, we extracted IQGAP2 mRNA expression data and the follow-up data on PC recurrence (BCR) from two independent datasets from cBioportal: TCGA provisional ($n=490$) and MSKCC ($n=140$). We then determined the cutoff points to separate the recurrent PCs from nonrecurrent tumors in both datasets using the Maximally Selected Rank Statistics (the *Maxstat* package in R) (Supplementary Figure 3). PCs with IQGAP2 mRNA expression < the respective cutoff point in each dataset were assigned a binary code "1" (cutoff point positive), and PCs with IQGAP2 mRNA expression ≥ the cutoff point were given "0" (cutoff point negative). In both cohorts, PCs with IQGAP2 mRNA expression below the cutoff point (cutoff point positive) were associated with a significant reduction in DFS compared to PCs expressing IQGAP2 above the cutoff point (cutoff point negative) (Figure 8). In the two independent cohorts, IQGAP2 mRNA expression was determined using two different approaches: RNA sequencing for the TCGA dataset and microarray analysis for the MSKCC cohort. Thus, the demonstration of association between PC recurrence and decreases in IQGAP2 mRNA expression in two independent cohorts in which IQGAP2 mRNA expression was measured with different experimental systems validated the relevance of IQGAP2 downregulation in PC recurrence.

Discussion

This report provides the first thorough characterization of IQGAP2 alterations during PC pathogenesis and progression. Consistent with previously reported increases in the IQGAP2 protein in low-grade
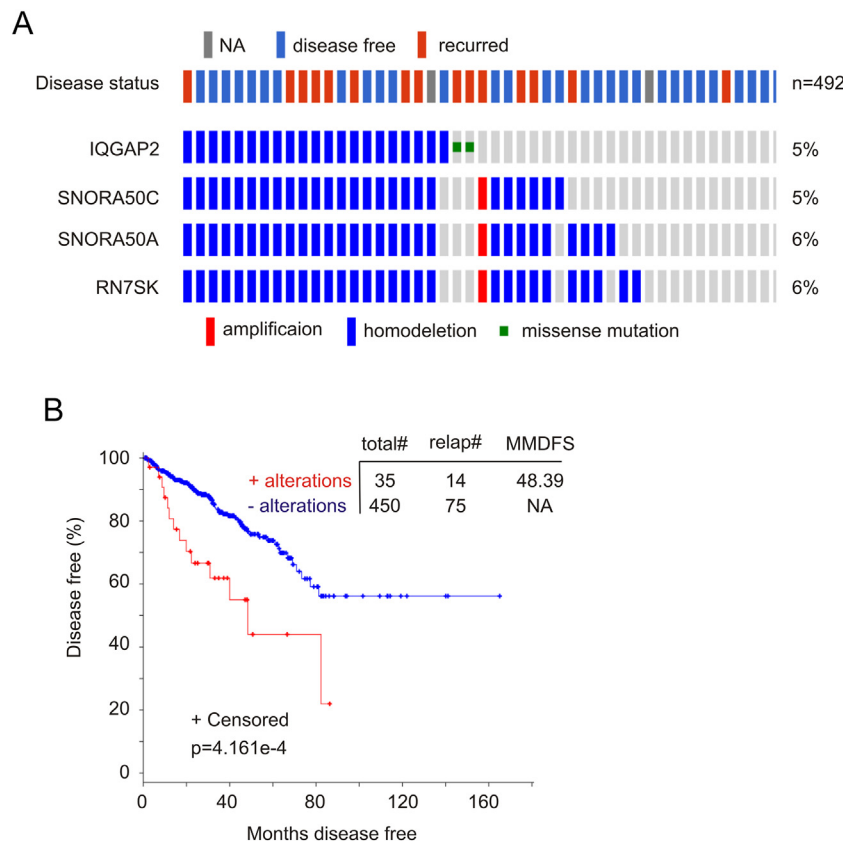

Figure 5. Genomic alterations in the *IQGAP2*, *SNORA50C*, *SNORA50A*, and *RN7SK* genes correlate with reductions in DFS. Data were extracted from the TCGA dataset within the cBioPortal database [19,20]. Genomic alterations in these genes (A) and their effects on DFS (B) were determined. Statistical analysis was performed using log-rank test. Total#: total number of cases; relap#: number of relapsed cases; MMDFS: median months of disease-free survival; NA: not available. Censored individuals are indicated; the number of censored individuals is the total individuals minus relapsed patients.
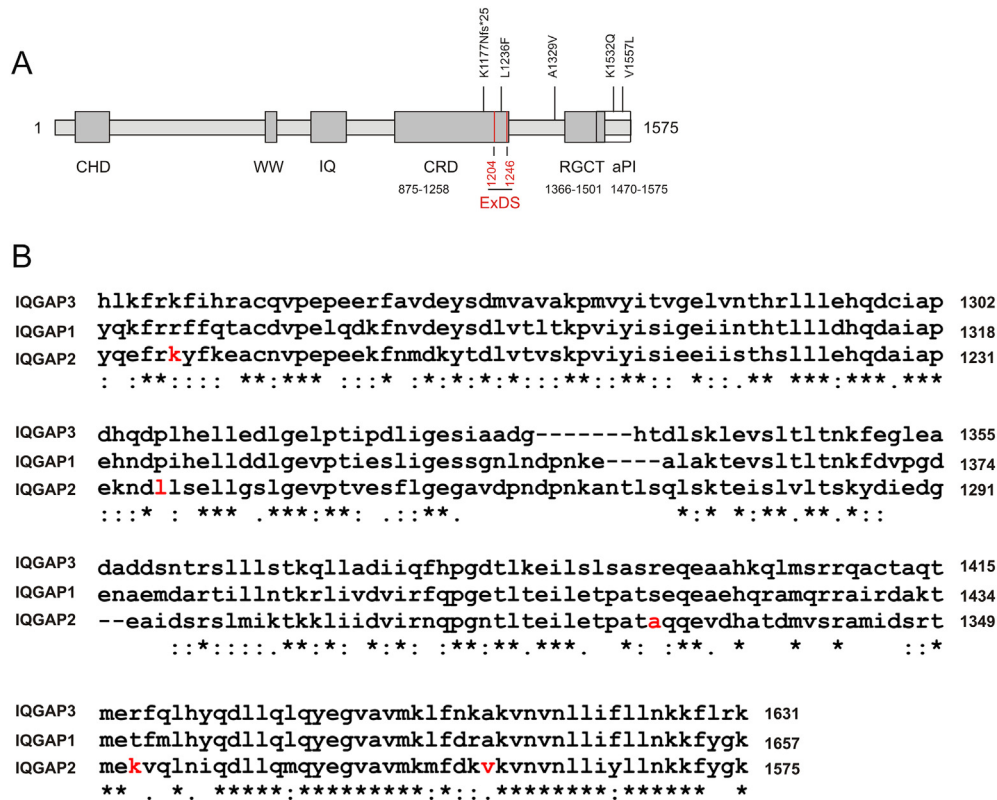
Figure 6. Clustering of mutations in a C-terminal region of IQGAP2. IQGAP2 mutation data were extracted from the TCGA, SU2C [26], and Broad/Cornell (2012) [27] datasets within the cBioPortal database [19,20]. (A) An illustration of IQGAP2 domain organization with sites of mutation indicated. The CRD contains "extra domain sequences" (ExDS) in two regions: residues 875-914 and 1204-1246 [30]; for simplicity, only one regions is shown. aPI is atypical phosphatidylinositol (3,4,5) binding domain [7]. CHD: calponin homology domain; GRD: RasGAP-related domain; and RGCT: RasGAP_C terminus. The locations of individual mutations are indicated. K1177Nfs*25: substitution of K117 with N and frame shift with a stop codon formed at position 25. (B) Alignment among IQGAP1-3 was determined using the Clustal Omega program of EMBL-EBI (http://www.ebi.ac.uk/Tools/msa/clustalo/). Only the regions containing five IQGAP2 mutations are included. Red residues indicate K1177, L1236, A1329, K1532, and V1557 for IQGAP2; these residues are mutated in PC.

PCs, we confirmed this elevation at the mRNA level in four relatively large and independent cohorts (Figure 1). More importantly, this elevation can diagnose PC with AUC values ranging from 0.7 to 0.8 (Figure 3). Considering that PSA is the only clinical biomarker used in PC diagnosis with an AUC approximately 0.57 [34], the elevation of IQGAP2 can be explored for PC diagnosis in future. This application is appealing as the elevation is likely a functional consequence of PC progression. Nonetheless, the mechanisms underlying IQGAP2 upregulation need to be elucidated in future.

Evidence suggests that deletion in the *IQGAP2* gene is a mechanism for its downregulation in high-grade PCs (Supplementary

Table 2). The deletion correlates with a reduction in DFS (*P*=.033, data not shown). Although the number of patients is very limited, the rapid kinetics of death in patients with metastatic PCs in which the *IQGAP2* gene was deleted (Supplementary Figure 2) supports a role of the deletion in promoting PC progression. It should be pointed out that in the cohort of 218 patients consisting of 181 primary tumors, no IQGAP2 mutations and CNV were detected [21] (see the MSKCC, Cancer Cell 2010 dataset within cBioPortal). Interestingly, there were also no SPOP mutations and CNV for SNORA50A, SNORA50C, and RN7SK (data not shown) in the MSKCC cohort, suggesting that the difference in *IQGAP2* genomic
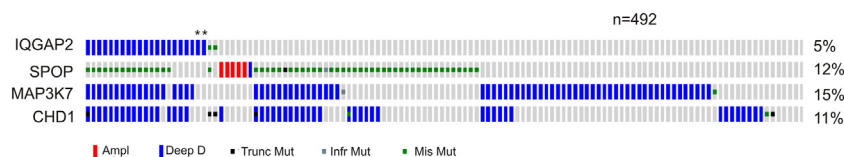

Figure 7. Prostate cancers with IQGAP2 genomic alterations are within the SPOP subtype of PC. Data were extracted from the TCGA dataset within the cBioPortal database [19,20]. Genomic alterations in the indicated genes are shown. Largely, only the tumors with the indicated changes are included. The co-occurrence between *IQGAP2* genomic changes with the indicated alterations in *SPOP*, *MAP3K7*, or *CHD1* was at *P*<.001 (Fisher's exact test) and log odds ratio >3.
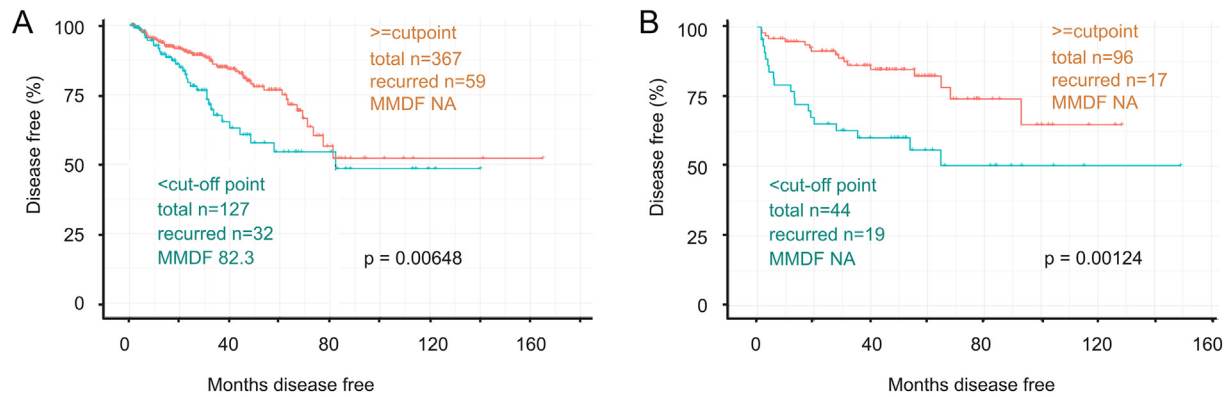
Figure 8. Downregulation of IQGAP2 mRNA expression is associated with a reduction in disease free survival in patients with prostate cancer. IQGAP2 mRNA data from the TCGA and MSKCC dataset (cBioPortal) were estimated for a cutoff point (see Supplementary Figure 3 for details). Kaplan-Meier survival analysis of PCs classified according to the cutoff point was performed for the TCGA (A) and MSKCC dataset (B). MMDF: median months disease free; NA: not available as MMDF not reached. Kaplan-Meier and log-rank tests were carried out with the R *survival* Package.

changes in both cohorts was likely due to differences in PC subtypes. Nonetheless, downregulation of IQGAP2 expression in both TCGA and MSKCC cohorts is associated with PC recurrence (Figure 8).

The co-occurrence of CNV for SNORA50A, SNORA50C, and RN7SK with the IQGAP2 genomic alterations (Table 2) suggests the noncoding RNAs coordinating with IQGAP2 in suppression of PC progression. The candidate genes regulated by these RNAs need future investigations. Since Cdk9 contributes to androgen receptor (AR) function via phosphorylating AR at serine 81 [35], RN7SK may repress AR signaling via inhibiting Cdk9 function [28,29]. Nonetheless, the observed co-changes in *IQGAP2*, *SNORA50A*, *SNORA50C*, and *RN7SK* genes may be developed into a diagnostic tool for PC recurrence.

Finally, *IQGAP2* GCN increases (amplification) can be detected in two CRPC datasets [36,37] within cBioPortal [19,20] (Supplementary Table 1). The function of this alteration and its clinical significance remain to be explored in the future.

Supplementary data to this article can be found online at https://doi.org/10.1016/j.tranon.2018.10.009.

References

[1] Ferlay J, Soerjomataram I, Dikshit R, Eser S, Mathers C, Rebelo M, Parkin DM, Forman D, and Bray F (2015). Cancer incidence and mortality worldwide: sources, methods and major patterns in GLOBOCAN 2012. *Int J Cancer* **136**, E359-386.

[2] Heidenreich A, Bastian PJ, Bellmunt J, Bolla M, Joniau S, van der Kwast T, Mason M, Matveev V, Wiegel T, and Zattoni F, et al (2014). EAU guidelines on prostate cancer. Part II: Treatment of advanced, relapsing, and castration-resistant prostate cancer. *Eur Urol* **65**, 467–479.

[3] Zaorsky NG, Raj GV, Trabulsi EJ, Lin J, and Den RB (2013). The dilemma of a rising prostate-specific antigen level after local therapy: what are our options? *Semin Oncol* **40**, 322–336.

[4] Semenas J, Allegrucci C, Boorjian SA, Mongan NP, and Persson JL (2012). Overcoming drug resistance and treating advanced prostate cancer. *Curr Drug Targets* **13**, 1308–1323.

[5] White CD, Brown MD, and Sacks DB (2009). IQGAPs in cancer: a family of scaffold proteins underlying tumorigenesis. *FEBS Lett* **583**, 1817–1824.

[6] Wang S, Watanabe T, Noritake J, Fukata M, Yoshimura T, Itoh N, Harada T, Nakagawa M, Matsuura Y, and Arimura N, et al (2007). IQGAP3, a novel effector of Rac1 and Cdc42, regulates neurite outgrowth. *J Cell Sci* **120**, 567–577.

[7] Dixon MJ, Gray A, Schenning M, Agacan M, Tempel W, Tong Y, Nedyalkova L, Park HW, Leslie NR, and van Aalten DM, et al (2012). IQGAP proteins reveal an atypical phosphoinositide (aPI) binding domain with a pseudo C2 domain fold. *J Biol Chem* **287**, 22483–22496.

[8] Xie Y, Kapoor A, Peng H, Cutz JC, Tao L, and Tang D (2015). IQGAP2 displays tumor suppression functions. *J Anal Oncology* **4**, 86–93.

[9] Hedman AC, Smith JM, and Sacks DB (2015). The biology of IQGAP proteins: beyond the cytoskeleton. *EMBO Rep* **16**, 427–446.

[10] Schmidt VA (2012). Watch the GAP: emerging roles for IQ motif-containing GTPase-activating proteins IQGAPs in hepatocellular carcinoma. *Int J Hepatol* **2012**, 958673.

[11] Smith JM, Hedman AC, and Sacks DB (2015). IQGAPs choreograph cellular signaling from the membrane to the nucleus. *Trends Cell Biol* **25**, 171–184.

[12] Jameson KL, Mazur PK, Zehnder AM, Zhang J, Zarnegar B, Sage J, and Khavari PA (2013). IQGAP1 scaffold-kinase interaction blockade selectively targets RAS-MAP kinase-driven tumors. *Nat Med* **19**, 626–630.

[13] Carmon KS, Gong X, Yi J, Thomas A, and Liu Q (2014). RSPO-LGR4 functions via IQGAP1 to potentiate Wnt signaling. *Proc Natl Acad Sci U S A* **111**, E1221-1229.

[14] Schmidt VA, Chiariello CS, Capilla E, Miller F, and Bahou WF (2008). Development of hepatocellular carcinoma in Iqgap2-deficient mice is IQGAP1 dependent. *Mol Cell Biol* **28**, 1489–1502.

[15] Gnatenko DV, Xu X, Zhu W, and Schmidt VA (2013). Transcript profiling identifies iqgap2(-/-) mouse as a model for advanced human hepatocellular carcinoma. *PLoS One* **8**e71826.

[16] White CD, Khurana H, Gnatenko DV, Li Z, Odze RD, Sacks DB, and Schmidt VA (2010). IQGAP1 and IQGAP2 are reciprocally altered in hepatocellular carcinoma. *BMC Gastroenterol* **10**, 125.

[17] Jin SH, Akiyama Y, Fukamachi H, Yanagihara K, Akashi T, and Yuasa Y (2008). IQGAP2 inactivation through aberrant promoter methylation and promotion of invasion in gastric cancer cells. *Int J Cancer* **122**, 1040–1046.

[18] Xie Y, Yan J, Cutz JC, Rybak AP, He L, Wei F, Kapoor A, Schmidt VA, Tao L, and Tang D (2012). IQGAP2, A candidate tumour suppressor of prostate tumorigenesis. *Biochim Biophys Acta* **1822**, 875–884.

[19] Cerami E, Gao J, Dogrusoz U, Gross BE, Sumer SO, Aksoy BA, Jacobsen A, Byrne CJ, Heuer ML, and Larsson E, et al (2012). The cBio cancer genomics portal: an open platform for exploring multidimensional cancer genomics data. *Cancer Discov* **2**, 401–404.

[20] Gao J, Aksoy BA, Dogrusoz U, Dresdner G, Gross B, Sumer SO, Sun Y, Jacobsen A, Sinha R, and Larsson E, et al (2013). Integrative analysis of complex cancer genomics and clinical profiles using the cBioPortal. *Sci Signal* **6** [pl1].

[21] Taylor BS, Schultz N, Hieronymus H, Gopalan A, Xiao Y, Carver BS, Arora VK, Kaushik P, Cerami E, and Reva B, et al (2010). Integrative genomic profiling of human prostate cancer. *Cancer Cell* **18**, 11–22.

[22] Grasso CS, Wu YM, Robinson DR, Cao X, Dhanasekaran SM, Khan AP, Quist MJ, Jing X, Lonigro RJ, and Brenner JC, et al (2012). The mutational landscape of lethal castration-resistant prostate cancer. *Nature* **487**, 239–243.

[23] Lapointe J, Li C, Higgins JP, van de Rijn M, Bair E, Montgomery K, Ferrari M, Egevad L, Rayford W, and Bergerheim U, et al (2004). Gene expression profiling identifies clinically relevant subtypes of prostate cancer. *Proc Natl Acad Sci U S A* **101**, 811–816.

[24] Tomlins SA, Mehra R, Rhodes DR, Cao X, Wang L, Dhanasekaran SM, Kalyana-Sundaram S, Wei JT, Rubin MA, and Pienta KJ, et al (2007). Integrative molecular concept modeling of prostate cancer progression. *Nat Genet* **39**, 41–51.

[25] Baca SC, Prandi D, Lawrence MS, Mosquera JM, Romanel A, Drier Y, Park K, Kitabayashi N, MacDonald TY, and Ghandi M, et al (2013). Punctuated evolution of prostate cancer genomes. *Cell* **153**, 666–677.

[26] Robinson D, Van Allen EM, Wu YM, Schultz N, Lonigro RJ, Mosquera JM, Montgomery B, Taplin ME, Pritchard CC, and Attard G, et al (2015). Integrative clinical genomics of advanced prostate cancer. *Cell* **161**, 1215–1228.

[27] Barbieri CE, Baca SC, Lawrence MS, Demichelis F, Blattner M, Theurillat JP, White TA, Stojanov P, Van Allen E, and Stransky N, et al (2012). Exome sequencing identifies recurrent SPOP, FOXA1 and MED12 mutations in prostate cancer. *Nat Genet* **44**, 685–689.

[28] Nguyen VT, Kiss T, Michels AA, and Bensaude O (2001). 7SK small nuclear RNA binds to and inhibits the activity of CDK9/cyclin T complexes. *Nature* **414**, 322–325.

[29] Yang Z, Zhu Q, Luo K, and Zhou Q (2001). The 7SK small nuclear RNA inhibits the CDK9/cyclin T1 kinase to control transcription. *Nature* **414**, 317–322.

[30] LeCour Jr L, Boyapati VK, Liu J, Li Z, Sacks DB, and Worthylake DK (2016). The structural basis for Cdc42-induced dimerization of IQGAPs. *Structure* **24** (9), 1499–1508.

[31] Cancer Genome Atlas Research N (2015). The molecular taxonomy of primary prostate cancer. *Cell* **163**, 1011–1025.

[32] Blattner M, Lee DJ, O'Reilly C, Park K, MacDonald TY, Khani F, Turner KR, Chiu YL, Wild PJ, and Dolgalev I, et al (2014). SPOP mutations in prostate cancer across demographically diverse patient cohorts. *Neoplasia* **16**, 14–20.

[33] Boysen G, Barbieri CE, Prandi D, Blattner M, Chae SS, Dahija A, Nataraj S, Huang D, Marotz C, and Xu L, et al (2015). SPOP mutation leads to genomic instability in prostate cancer. *elife* **4**.

[34] van Gils MP, Hessels D, van Hooij O, Jannink SA, Peelen WP, Hanssen SL, Witjes JA, Cornel EB, Karthaus HF, and Smits GA, et al (2007). The time-resolved fluorescence-based PCA3 test on urinary sediments after digital rectal examination; a Dutch multicenter validation of the diagnostic performance. *Clin Cancer Res* **13**, 939–943.

[35] Chen S, Gulla S, Cai C, and Balk SP (2012). Androgen receptor serine 81 phosphorylation mediates chromatin binding and transcriptional activation. *J Biol Chem* **287**, 8571–8583.

[36] Beltran H, Prandi D, Mosquera JM, Benelli M, Puca L, Cyrta J, Marotz C, Giannopoulou E, Chakravarthi BV, and Varambally S, et al (2016). Divergent clonal evolution of castration-resistant neuroendocrine prostate cancer. *Nat Med* **22**, 298–305.

[37] Kumar A, Coleman I, Morrissey C, Zhang X, True LD, Gulati R, Etzioni R, Bolouri H, Montgomery B, and White T, et al (2016). Substantial interindividual and limited intraindividual genomic diversity among tumors from men with metastatic prostate cancer. *Nat Med* **22**, 369–378.